

Grease-ice thickness parameterization

Lars H. SMEDSRUD

*Bjerknes Centre for Climate Research, c/o Geophysical Institute, Allégaten 70, NO-5007 Bergen, Norway
E-mail: Lars.Smedsrud@uni.no*

ABSTRACT. Grease ice is a mixture of sea water and frazil ice crystals forming in Arctic and Antarctic waters. The initial grease-ice cover, or the grease ice forming during winter in leads and polynyas, may therefore have mixed properties of water and ice. Most sea-ice models use a lower thickness limit on the solid sea ice, representing a transition from grease ice to solid ice. Before grease ice solidifies it is often packed into a layer by the local wind. Existing field measurements of grease ice are compared and used to evaluate a new thickness parameterization including the drag from the wind as well as the ocean current. The measurements support a scaling of the wind drag and the back pressure from the grease-ice layer using a nonlinear relation. The relation is consistent with an increasing grease-ice thickness towards a solid boundary. Grease-ice data from Storfjorden, Svalbard, confirm that tidal currents are strong enough to add significant drag force on the grease ice. A typical wind speed of only 10 m s^{-1} results in a 0.3 m thick layer of grease ice. Tidal currents of 0.5 m s^{-1} will pack the grease ice further towards a stagnant boundary to a mean thickness of 0.8 m.

INTRODUCTION

Grease ice forms when turbulent sea water at the freezing point is directly cooled by the atmosphere. Such conditions are often found in Arctic and Antarctic waters, especially in polynyas and leads. Grease ice is a mixture of free-floating frazil ice crystals and sea water, and observations are limited because of the difficulty of reaching and working in these situations. More observations of grease and frazil ice are available from laboratory investigations (Martin and Kauffman, 1981; Daly and Colbeck, 1986; Smedsrud, 2001).

Sea ice may be divided by its texture into columnar and granular ice. Columnar ice is the 'normal' solid sea ice frozen by heat conduction through an already existing ice cover. Granular ice is most commonly frazil and grease ice that has congealed at a later stage. In the Weddell Sea, Antarctica, granular ice has been found in similar volumes to columnar ice ($\sim 30\%$ of the total sea-ice volume; Eicken and Lange, 1989). The remaining ice is of a mixed type, probably caused by dynamic deformation. In the Arctic, granular ice of frazil- or grease-ice origin is less frequent (typically $\sim 20\%$ of the ice volume; Eicken and others, 1995).

Polynyas are known to have important climatic impacts on the polar ocean and atmosphere (Morales Maqueda and others, 2004). With reduced Arctic summer ice cover (Serreze and others, 2007), and consequently increased seasonal ice growth, Arctic granular ice will likely become more common in the future. This increases the importance of incorporating grease-ice processes in general circulation models (GCMs) which aim to predict the future Arctic ice cover. A necessary first step in building such a parameterization is predicting the grease-ice thickness given the larger-scale forcing.

The following section summarizes relevant grease-ice properties based on field observations. A force balance between the wind and ocean drag and the back pressure from the grease-ice layer is then presented. The new thickness parameterization is tested and sensitivities to some parameters are given before conclusions are drawn.

FIELD OBSERVATIONS

In the natural environment, individual frazil crystals grow and are mixed downwards by local turbulence until their buoyancy becomes stronger than the downward diffusion. This forms the grease-ice layer that gradually covers the open ocean (Fig. 1). This grease ice damps the local turbulence and surface waves, and may gradually start to congeal from the top downwards. The number of available data is limited (Martin and Kauffman, 1981; Smedsrud and Skogseth, 2006) but sufficient for evaluation of a new thickness parameterization.

Arctic grease ice has a minimum bulk salinity of 21.5 psu (Smedsrud and Skogseth, 2006). The salinity range is therefore between this minimum and that of the original sea water. This implies that the grease ice consists of a major portion of sea water and a smaller portion of frazil ice crystals. The frazil crystals are pure fresh water, and the calculated range in frazil volume fraction of the grease ice is 16–32% (Smedsrud and Skogseth, 2006). This concentration may vary in time depending on heat flux, wave motion, age of the grease ice and other processes.

The mean frazil volume concentration of the grease ice found around Svalbard (Smedsrud and Skogseth, 2006) was 25.3%. This is within the range of earlier values from laboratory experiments. A range of 14–29% is consistent with the values in Martin and Kauffman (1981), when a correction for the sea-water content of the grease ice is made as noted by Smedsrud and Skogseth (2006). A constant frazil ice concentration of 25% is therefore a reasonable approximation and will be used here. This implies a bulk grease-ice density of $\rho_g = 0.75\rho_w + 0.25\rho_i = 1000 \text{ (kg m}^{-3}\text{)}$ using a sea-water density of $\rho_w = 1027 \text{ kg m}^{-3}$ and an ice density of $\rho_i = 920 \text{ kg m}^{-3}$.

Grease ice therefore has a surface temperature close to that of salt water at the freezing point. Observations of the grease-ice-covered surface layers show that the temperature remains within $\pm 0.040^\circ\text{C}$ of the freezing point for the upper ocean salinity (Skogseth and others, 2009).

Given a continued heat loss to the atmosphere, grease ice congeals with time. If waves are present this initial congealed

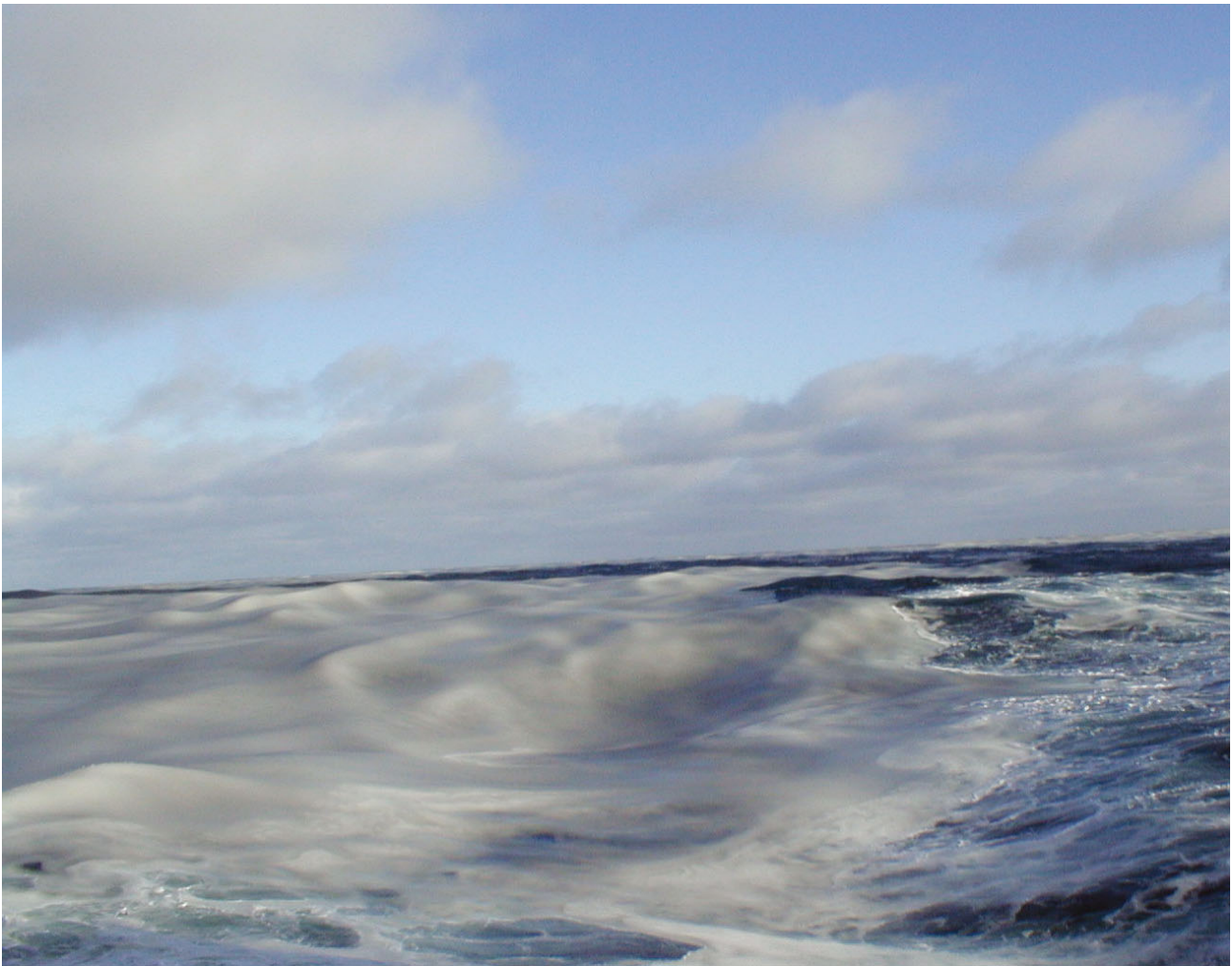


Fig. 1. A layer of grease ice observed in open-ocean conditions on 28 March 2007. The grease ice covered several kilometres along the KV *Svalbard* ship track between Hopen and Bear Island in the northern Barents Sea. The grease-ice layer damps high-frequency wind waves, so that the water surface appears 'greasy'.

ice will be pancake ice floes of varying size and thickness (Wadhams and Wilkinson, 1999). Grease ice is sometimes pushed or transported below thicker ice by external forces such as wind, sea-ice motion or ocean currents. During the period of observations in Storfjorden, Svalbard (Smedsrud and Skogseth, 2006), a fast-ice cover was attached to nearby islands and the tidally dominated ocean current varied from 2.2 to 41.5 cm s^{-1} during the grease-ice sampling. The varying current speed did not correspond directly to the grease-ice thickness at the given time and place, but the mean speed at 5 m depth was 21.5 cm s^{-1} (used later).

Grease ice forms instantly in open water due to net ocean–air heat flux. Depending on the wind, air temperature, currents and waves this grease-ice layer may be present for some time. The ice is then the 'greasy' surface layer from which it is named (Fig. 1). Similar grease ice has been observed on many occasions during fieldwork around Svalbard.

GREASE-ICE THICKNESS FORCE BALANCE

The maximum grease-ice thickness has previously been termed the collection thickness, and this parameter plays an important role in polynya models (Biggs and Willmott, 2004). The fetch, the effective distance for wind forcing along the

wind direction, has also been incorporated. The collection thickness is expected to decrease for a smaller fetch (Alam and Curry, 1998). The fetch is not easily defined in a partly ice-covered ocean, and is not available for larger-scale ice–ocean models. As noted by Bauer and Martin (1983), such a fetch would vary constantly due to the relative motion of the sea-ice floes and the wind surrounding the grease ice.

The parameterization suggested here relates directly to the force packing the grease ice towards a neighbouring sea-ice floe. It also makes use of basic forcing available in any ocean model with a sea-ice component: the stress from the wind above and from the ocean current below.

Figure 2 depicts an idealized, but typical, horizontal distribution of a grease-ice layer. Wind (U_a) and the ocean current (U_w) push the grease ice towards the pack ice. The total length of the grease-ice layer along the wind and current is L . At x the grease-ice thickness is $h_g(x)$. In laboratory data for pancake ice (Dai and others, 2004), a maximum thickness or equilibrium thickness has been found. Field observations (Smedsrud and Skogseth, 2006) confirm this to some extent, but we make no assumption of a maximum thickness here.

Each frazil-ice crystal in the grease-ice layer (Fig. 2) is subject to a water drag force, collision forces between ice crystals, buoyancy and gravity. The analogy with single pancakes in a pancake-ice field is clear (Dai and others,

2004), but the packing force for the grease ice is the wind and current drag and not the waves. If there are no wind or currents the frazil crystals and grease-ice layer will spread evenly over the open-water area, and solidification will start rapidly given a continued heat loss. Heat loss from the solid pack ice is small due to the slow heat conduction through thicker ice; given a cold atmosphere, heat fluxes are generally large over an open or grease-ice-covered ocean (Fig. 2).

The resistance force (per unit width, N m^{-1}) from a granular layer towards further thickening by the packing force (consider pushing a vertical wall towards a pile of sand) is defined (Dai and others, 2004):

$$F_r = K_r h_g^2, \quad (1)$$

where

$$K_r = \frac{1}{2} \left(\frac{1 + \sin \phi}{1 - \sin \phi} \right) (1 - n) \rho_g g \left(1 - \frac{\rho_g}{\rho_w} \right), \quad (2)$$

to be evaluated from field data (N m^{-3}). Here ϕ is an internal friction angle which is a function of both the inter-particle friction and the packing geometry, n is the bulk porosity of frazil in the grease ice, and g is the gravitational constant. For small friction angles of $\phi < 10^\circ$ and frazil-ice concentration of $n > 0.25$, the resistance force (Equation (1)) is given by $K_r \sim 100$.

The grease-ice layer experiences a packing force from the wind and current: $\tau_p = \tau_a + \tau_w$. The wind stress (N m^{-2}),

$$\tau_a = \rho_a C_a (U_a - U_i)^2,$$

may be estimated using air density $\rho_a = 1.4 \text{ kg m}^{-3}$, a normal open-ocean drag coefficient $C_a = 1.3 \times 10^{-3}$ (Smith, 1988) and the wind velocity at 10 m height U_a (m s^{-1}). The ocean stress,

$$\tau_w = \rho_w C_w (U_i - U_w)^2,$$

is calculated from the mixed-layer current, U_w (m s^{-1}), in a similar way. A drag coefficient for the ocean on the grease-ice layer of $C_w = 6.0 \times 10^{-3}$ is used, consistent with standard quadratic drag (Steiner, 2001).

Along any section of the grease ice ($0 \leq x \leq L$) there will be a force balance (N m^{-1}):

$$\delta F_r = \delta K_r h_g^2 = K_r \delta h_g^2 = \tau_p \delta x, \quad (3)$$

where

$$h_g^2 = \int_0^L \frac{\tau_p}{K_r} dx \quad (4)$$

(measured in m^2). This follows Pariset and Hausser (1961) and the force balance in a wide river (personal communication from H.T. Shen, 2009). To proceed and find the grease-ice thickness as a function of the wind, we first assume $U_i = 0$ and $\tau_w = 0$, and obtain:

$$h_g^2(x) = \frac{\rho_a C_a}{K_r} U_a^2 x \quad (5)$$

or

$$h_g(x) = \sqrt{\frac{\rho_a C_a}{K_r}} U_a \sqrt{x}. \quad (6)$$

Any given wind drag will thus create a profile of grease ice, but the total amount of grease ice is determined thermodynamically by the heat loss, F_{tot} , over a given time, Δt , and the length of the open water along the wind direction, L_{lead} . The area of open water (L_{lead} multiplied by

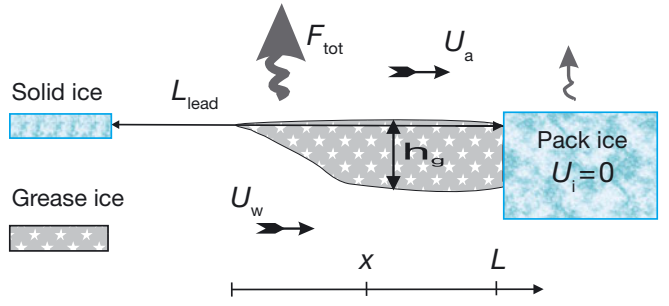


Fig. 2. An idealized layer of grease ice pushed against a larger floe of stagnant pack ice. Heat flux from the area of open water and grease ice is combined as F_{tot} and is larger than the heat flux through the solid ice.

width) where the heat flux F_{tot} is effective and grease ice is produced is different from the area covered by grease ice (L multiplied by width). The wind (and current) advect grease ice along and $L \leq L_{\text{lead}}$. The energy lost (per unit width) is $F_{\text{tot}} \Delta t L_{\text{lead}}$ (J m^{-1}) and will be taken as a given value here. The lost energy is proportional to a grease-ice volume, V_g (m^2 per unit width) through the latent heat of freezing of ice ($L_i = 3.35 \times 10^5 \text{ J kg}^{-1}$) and the ice density. We also correct for the 75% volume fraction of unfrozen water in the grease ice, yielding

$$V_g = \frac{F_{\text{tot}} \Delta t L_{\text{lead}}}{0.25 L_i \rho_i}. \quad (7)$$

The total grease-ice volume per unit width is thus

$$\begin{aligned} V_g &= \int_0^L h_g dx = \int_0^L \sqrt{\frac{\rho_a C_a}{K_r}} U_a \sqrt{x} dx \\ &= \left[\frac{2}{3} \sqrt{\frac{\rho_a C_a}{K_r}} U_a x^{3/2} \right]_{x=0}^{x=L} = \frac{2}{3} \sqrt{\frac{\rho_a C_a}{K_r}} U_a L^{3/2}. \end{aligned} \quad (8)$$

An expression for L may then be found:

$$L = \left[\frac{3}{2} \frac{V_g}{U_a} \sqrt{\frac{K_r}{\rho_a C_a}} \right]^{2/3}. \quad (9)$$

Finally, an expression for the mean grease-ice thickness, $\overline{h_g}$, as a function of wind speed is obtained by substituting Equation (9) into Equation (8):

$$\overline{h_g} = \frac{1}{L} \int_0^L h_g dx = \frac{1}{L} V_g = (V_g)^{1/3} \left(\frac{2}{3} \sqrt{\frac{\rho_a C_a}{K_r}} U_a \right)^{2/3}. \quad (10)$$

For a given heat flux, F_{tot} , the mean grease-ice thickness is therefore proportional to $U_a^{2/3}$. In general, F_{tot} also increases with U_a . This relation between grease-ice thickness and wind (Equation (10)) will later be compared to earlier formulations and field data, where a 'typical' heat flux value is found useful.

An important special situation is the absence of both wind and currents. In this case, the sensible and latent heat losses will be small as they also scale with the wind, but F_{tot} could for example still be large due to outgoing longwave radiation. The heat loss will also produce ice in this case, but h_g will still be zero from Equation (10). This is also consistent with observations, and the sea ice formed under such quiet conditions is 'normal' columnar ice.

If the solid, thick, sea ice in Figure 2 is drifting ($U_i \neq 0$) or there is a significant drag from the ocean currents

($\tau_w \neq 0$) these will also affect the grease-ice thickness. A full implementation in a three-dimensional (3-D) model will have to account for the wind direction in Equation (10) and the orientation of the ice edge. Here a two-dimensional (2-D) approach is taken, so that the wind and currents are perpendicular to the solid ice edge. In this setting, the ice drift, U_i , will simply add relative speed and U_a should be replaced by $U_a - U_i$ in Equation (10).

For a case with significant drag from the ocean current below, τ_w makes a contribution to the grease-ice thickness as

$$h_g(x) = \sqrt{\frac{\rho_a C_a}{K_r}} U_a \sqrt{x} + \sqrt{\frac{\rho_w C_w}{K_r}} U_w \sqrt{x} \quad (11)$$

which implies that

$$\bar{h}_g = \frac{2}{3} (V_g)^{\frac{1}{3}} \left[\sqrt{\frac{\rho_a C_a}{K_r}} U_a + \sqrt{\frac{\rho_w C_w}{K_r}} U_w \right]^{\frac{2}{3}}. \quad (12)$$

DISCUSSION

Early sea-ice modellers realized that open-water ice growth is a key element of any sea-ice model (Hibler, 1979). The new ice volume grown in open water is transferred into thicker solid sea ice that lowers further heat loss and thereby limits the open-water area. Hibler (1979) established such a relationship through a demarcation between thin and thick ice of $h_0 = 0.5$ m, and used a seasonal growth rate estimate of 0.1 m d^{-1} for winter conditions. This is comparable to a total heat flux of 273 W m^{-2} using a normal solid ice salinity of 8 psu. With the advent of more than one ice category this has become more complicated, but the general assumption still used is that open-water heat loss produces ice growth instantly (in less than one time-step) and this is converted to solid ice. The ice growth described by the model prevents the ocean from becoming supercooled. The surface supercooling of 0.037°C found by Skogseth and others (2009) is probably close to the maximum occurring under most natural conditions. This model assumption of no supercooling is therefore not correct, but is a reasonable approximation for a large-scale model.

The rapid open-water ice growth can, under natural conditions, only take place through frazil-ice growth, producing the grease-ice layer. A difficulty then arises when distributing the new volume of ice between growth in thickness and growth in area. In Hibler (1979), this is related to the demarcation thickness, $h_0 = 0.5$ m, and the frozen volume is transferred from water to the thick ice category (well above 0.5 m thickness). Mellor and Kantha (1989) reported a tuning parameter $\Phi_F = 4$, dividing open-water solid-ice growth between increases in sea-ice thickness and in sea-ice area. Sensitivity studies and tuning have been performed, comparing model results to present-day Arctic Ocean sea ice.

Polynya models use a 'frazil collection thickness', the maximum thickness of the frazil layer at the polynya edge (Drucker and others, 2003). This is essentially the same as the demarcation thickness used by Hibler (1979), the transition value between open water with frazil ice (the grease-ice layer) and the solid sea ice in the pack ice.

A recently updated sea-ice model (LIM3) forms new ice in open water with a thickness of $0.05 < h_0 < 0.15$ m (Vancoppenolle and others, 2010). This h_0 depends nonlinearly on wind speed, ice velocity and pack-ice

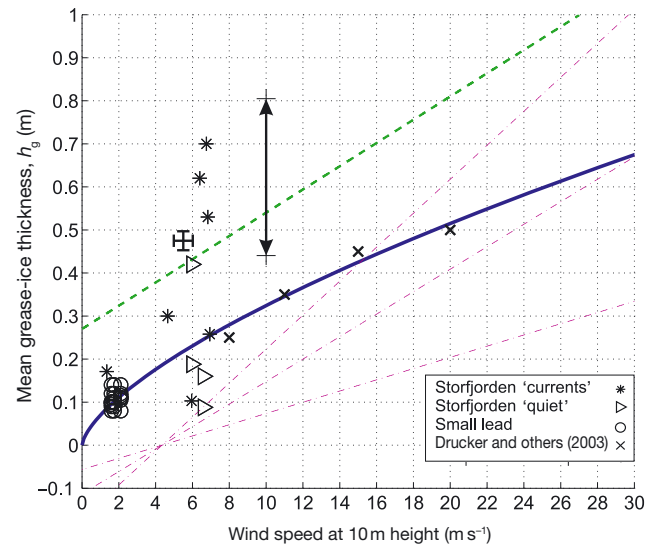


Fig. 3. Mean grease-ice thickness along the wind direction as a function of wind speed. The solid curve is the new relationship for h_g . Previous relations from Winsor and Björk (2000, green dashed line) and Alam and Curry (1998, magenta dash-dotted lines) are also included. Individual measurements from Smedsrud and Skogseth (2006) and Drucker and others (2003) are shown by symbols. The effect of an additional current speed of $0.1\text{--}0.5 \text{ m s}^{-1}$ on the grease-ice thickness is indicated at 10 m s^{-1} wind by the arrow. Error bars are plotted for $h_g = 0.48 \text{ m}$ and a 5.5 m s^{-1} wind. This value is the average for the Storfjorden current data produced by an additional current of 0.21 m s^{-1} .

thickness, and is based on a theoretical polynya model (Biggs and others, 2000) validated with small-scale laboratory experiments (Martin and Kauffman, 1981). No further discussion of how the grease ice solidifies into pancake ice, or other types of solid ice, will be given here. A better parameterization of the grease-ice thickness is a first and necessary step to model such a transition.

A linear dependence between grease-ice thickness and wind speed has been suggested (Alam and Curry, 1998). The relation used by Winsor and Björk (2000) for the collection depth, h_c (m), is also linear:

$$h_c = 0.27 + 0.027 | U_a. \quad (13)$$

Here a 25% pure ice fraction has been accounted for so that h_c would be the observed grease-ice thickness. Winsor and Björk (2000) thus suggest a constant lower bound of the grease-ice thickness of 0.27 m , increasing to over 1.0 m at wind speeds above 27 m s^{-1} as shown in Figure 3.

Based on a large number of field observations from the 'small lead' (Fig. 3) with wind speed $\sim 2 \text{ m s}^{-1}$ (Smedsrud and Skogseth, 2006), it is clear that the assumption of a grease-ice thickness linearly dependent on wind speed is invalid. Grease ice forms at a low wind speed, contradictory to the Alam and Curry (1998) formulae that need a threshold of 4 m s^{-1} . In addition, contradictory to the Winsor and Björk (2000) relation, the grease-ice thickness is close to 0.1 m at low wind speed and not over 0.2 m . A better linear relationship could be formulated, but the data points from Storfjorden with up to 0.7 m of grease ice in 7 m s^{-1} winds would still be unexplained.

Grease-ice data from Storfjorden cover wind speeds up to 7 m s^{-1} (Smedsrud and Skogseth, 2006), but those from Drucker and others (2003) have values up to 14 m s^{-1}

(Fig. 3). The data and Equation (10) show a good fit using values of $K_r = 100.0$ and $V_g = 40.0$. The low-wind-speed data are well represented in Figure 3. The benchmark grease-ice value of 0.3 m forced by a 10 m s^{-1} wind (and a 500 m fetch) from Bauer and Martin (1983) is also very close to the proposed mean grease-ice thickness as a function of wind speed (Fig. 3).

The data points in Figure 3 are from different locations and atmospheric conditions; it is therefore surprising that the same values of F_{tot} can be used. Given that the water is at the freezing point and that the wind brings cold dry air from the layer above a fairly homogeneous Arctic sea ice, an equilibrium situation does not seem totally unreasonable.

The heat loss used by Hibler (1979) for mean winter conditions (273 W m^{-2}) produced 0.1 m of normal solid sea ice in a day. The value for grease-ice volume used here of $V_g = 40.0$ implies a range in heat fluxes dependent on L_{lead} in Equation (7). A similar daily heat flux to that of Hibler (1979) implies an $L_{\text{lead}} = 130$. The same grease-ice volume ($V_g = 40$) may be produced over a longer stretch of open water with a smaller corresponding heat flux. A range of $500 \leq L_{\text{lead}} \leq 1000$ matches $71 \geq F_{\text{tot}} \geq 35$ to produce the same V_g . In the following calculations, values of $V_g = 40.0$ and $K_r = 100.0$ are used.

The additional drag from the currents in Storfjorden increases the grease-ice thickness. Using a mean observed current of 0.21 m s^{-1} in Equation (12), in addition to the mean observed wind of 5.5 m s^{-1} , yields an expected grease-ice thickness of 0.48 m. As shown in Figure 3, this is in good agreement with observations with a range of 0.1–0.7 m grease-ice thickness (Smedsrud and Skogseth, 2006). An exact agreement is not expected because of several factors. The current meter was located 1–2 km away from the sampled grease-ice thickness and measured a varying tidal speed of 0.02 – 0.42 m s^{-1} . A similar situation occurred for the wind speed: during the day of grease-ice sampling, winds of 1.3 – 6.6 m s^{-1} at 10 m height were calculated from measurements recorded at a 5 m high meteorological mast 1–3 km away (Smedsrud and Skogseth, 2006).

Two thickness profiles exist (Smedsrud and Skogseth, 2006) and may be compared to Equation (6). The difference in wind speed is quite small (5.95 m s^{-1} compared to 6.58 m s^{-1}), but a thicker profile is indicated for a stronger wind (Fig. 4). The scatter is significant but may be caused by differences in ocean current, among other factors. The effect of a 0.15 m s^{-1} current is comparable to a wind of 9 m s^{-1} . The thickness profiles in Figure 4 (from Equation (6)) are not dependent on V_g and are therefore a good validation for $K_r = 100$. Values of grease-ice resistance of $K_r < 50$ give effective packing and a thicker grease layer than actually observed. Values of grease-ice resistance of $K_r > 200$ predict thinner grease ice than observed. Reasonable values have therefore been found for K_r , F_{tot} and L_{lead} and, despite the limited number of observations, a consistent set of values has been determined.

In a high-resolution model study, Kämpf and Backhaus (1999) found that convection-induced surface currents increased the frazil thickness to several metres. This reproduced streaks of frazil, often observed in freezing polar waters, and confirms that surface currents influence the grease-ice layer. It is clear that ocean currents also influence the grease-ice layer; from Equation (12), $U_a = 10.0$ and $U_w = 0.5$ results in an increase of h_g up to 0.80 m (Fig. 3).

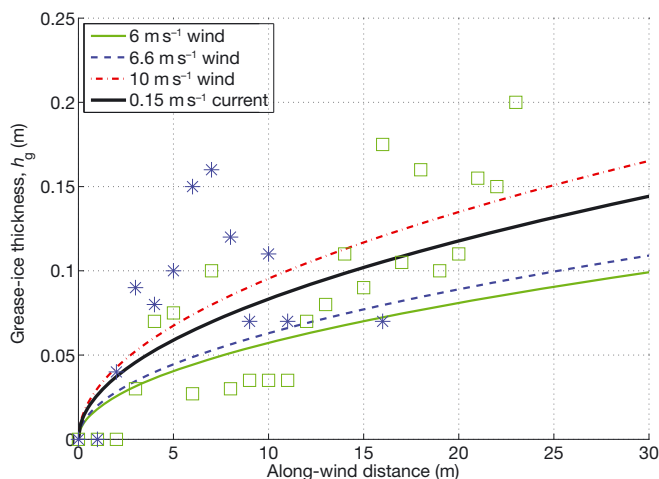


Fig. 4. Grease-ice thickness along the wind or current direction. The thickness profile resulting from a 6 m s^{-1} wind may be compared to the observed profile of grease-ice thickness depicted using green squares, while the 6.6 m s^{-1} profile may be compared to that depicted using blue stars.

SENSITIVITY

Drag coefficients depend on waves and surface roughness, and will have different values for an open ocean and one covered by grease ice. No values for a grease-ice-covered ocean have been found, but the sensitivity towards a varying C_a in Equation (12) can be tested. Doubling the atmospheric drag to $C_a = 2.6 \times 10^{-3}$ increases the expected grease-ice thickness for 30 m s^{-1} winds from 0.67 m to 0.84 m (Fig. 3). Similarly, it decreases to 0.53 m for $C_a = 0.65 \times 10^{-3}$.

A range of values for K_r (Equation (1)) was also tested in comparison to the grease-ice observations. Increasing the resistance creates a thinner grease-ice layer as expected. For a 30 m s^{-1} wind in Figure 3, $K_r = 200$ creates 0.53 m of grease ice. Likewise, a reduction in resistance to $K_r = 50$ generates a grease-ice thickness as large as 0.83 m.

The grease-ice thickness measurements have an accuracy of $\pm 0.01 \text{ m}$ (Smedsrud and Skogseth, 2006). In the wind relation (Equation (10)), this translates to an uncertainty in wind speed of $\pm 0.3 \text{ m s}^{-1}$. This is close to the instrumental accuracy (Aanderaa Wind Speed Sensor 2740: ± 0.2 – 0.6 m s^{-1}). In the relation including ocean currents (Equation (12)), $\pm 0.01 \text{ m}$ in grease-ice thickness compares to a current speed of $\pm 0.01 \text{ m s}^{-1}$. The accuracy of the current meter (Aanderaa RDCP 600) used was $\pm 0.005 \text{ m s}^{-1}$ (Skogseth and others, 2008). Error bars in Figure 3 have therefore been estimated as $\pm 0.5 \text{ m s}^{-1}$ for wind speed, $\pm 0.1 \text{ m s}^{-1}$ for current speed and $\pm 0.01 \text{ m}$ for grease-ice thickness.

CONCLUSION

A new parameterization of grease-ice thickness forced by wind and currents has been formulated. The relations are nonlinear, scale with wind and current speed as $U^{2/3}$ and predict existing grease-ice field data well. A 2-D approach is taken, with winds and ocean currents perpendicular to an ice edge. The new relation may be used in both polynya and sea-ice modelling. For a typical wind speed of 10 m s^{-1} , a mean grease-ice thickness of 0.3 m is predicted. The grease-ice thickness increases steadily from zero at the

upwind (upstream) end along the wind (current) direction. The grease-ice thickness increases to 0.2 m over the first 30 m and the layer is ~ 100 m long. The relation has low sensitivity to varying drag coefficients; a range in heat fluxes and lengths of open water may produce grease-ice volumes matching the parameterization.

An ocean current of 0.2 m s^{-1} packing the grease-ice layer towards a stagnant boundary will increase the grease-ice thickness by ~ 0.4 m and ~ 0.2 m for low and high wind speeds, respectively. A maximum grease-ice thickness of ~ 1 m results from 30 m s^{-1} wind speed and a 0.5 m s^{-1} current.

ACKNOWLEDGEMENTS

We thank Hayley Shen and Hung Tao Shen for guidance on the scaling of the force balance. This work was completed as part of the Bipolar Atlantic Thermohaline Circulation (BIAC) and NorClim projects funded by the Research Council of Norway. We thank P. Langhorne (scientific editor), M. Williams and an anonymous reviewer for helpful comments on the paper. This is publication No. A303 from the Bjerknes Centre for Climate Research.

REFERENCES

- Alam, A. and J.A. Curry. 1998. Evolution of new ice and turbulent fluxes over freezing winter leads. *J. Geophys. Res.*, **103**(C8), 15,783–15,802.
- Bauer, J. and S. Martin. 1983. A model of grease ice growth in small leads. *J. Geophys. Res.*, **88**(C5), 2917–2925.
- Biggs, N.R.T. and A.J. Willmott. 2004. Unsteady polynya flux model solutions incorporating a parameterization for the collection thickness of consolidated new ice. *Ocean Model.*, **7**(3–4), 343–361.
- Biggs, N.R.T., M.A. Morales Maqueda and A.J. Willmott. 2000. Polynya flux model solutions incorporating a parameterization for the collection thickness of consolidated new ice. *J. Fluid Mech.*, **408**, 179–204.
- Dai, S., H.H. Shen, M.A. Hopkins and S.F. Ackley. 2004. Wave rafting and the equilibrium pancake ice cover thickness. *J. Geophys. Res.*, **109**(C7), C07023. (10.1029/2003JC002192.)
- Daly, S.F. and S.C. Colbeck. 1986. Frazil ice measurements in CRREL's flume facility. In *Proceedings of the 8th International Symposium on Ice, 18–22 August 1986, Iowa City, Iowa*. Iowa City, IA, International Association for Hydraulic Research, 427–438.
- Drucker, R., S. Martin and R. Moritz. 2003. Observations of ice thickness and frazil ice in the St. Lawrence Island polynya from satellite imagery, upward looking sonar, and salinity/temperature moorings. *J. Geophys. Res.*, **108**(C5), 3149. (10.1029/2001JC001213.)
- Eicken, H. and M.A. Lange. 1989. Development and properties of sea ice in the coastal regime of the southeastern Weddell Sea. *J. Geophys. Res.*, **94**(C6), 8193–8206.
- Eicken, H., M. Lensu, M. Leppäranta, W.B. Tucker, III, A.J. Gow and O. Salmela. 1995. Thickness, structure and properties of level summer multi-year ice in the Eurasian sector of the Arctic Ocean. *J. Geophys. Res.*, **100**(C11), 22,697–22,710.
- Hibler, W.D., III. 1979. A dynamic thermodynamic sea ice model. *J. Phys. Oceanogr.*, **9**(7), 815–846.
- Kämpf, J. and J.O. Backhaus. 1999. Ice–ocean interactions during shallow convection under conditions of steady winds: three-dimensional numerical studies. *Deep-Sea Res. II*, **46**(6–7), 1335–1355.
- Martin, S. and P. Kauffman. 1981. A field and laboratory study of wave damping by grease ice. *J. Glaciol.*, **27**(96), 283–313.
- Mellor, G.L. and L. Kantha. 1989. An ice–ocean coupled model. *J. Geophys. Res.*, **94**(C8), 10,937–10,954.
- Morales Maqueda, M.A., A.J. Willmott and N.R.T. Biggs. 2004. Polynya dynamics: a review of observations and modeling. *Rev. Geophys.*, **42**(1), RG1004. (10.1029/2002RG000116.)
- Pariset, E. and R. Hausser. 1961. Formation and evolution of ice covers on rivers. *Trans. Eng. Inst. Can.*, **5**, 41–49.
- Serreze, M.C., M.M. Holland and J. Stroeve. 2007. Perspectives on the Arctic's shrinking sea-ice cover. *Science*, **315**(5818), 1533–1536.
- Skogseth, R., L.H. Smedsrud, F. Nilsen and I. Fer. 2008. Observations of hydrography and downflow of brine-enriched shelf water in the Storfjorden polynya. *J. Geophys. Res.*, **113**(C8), C08049. (10.1029/2007JC004452.)
- Skogseth, R., F. Nilsen and L.H. Smedsrud. 2009. Supercooled water in an Arctic polynya: observations and modeling. *J. Glaciol.*, **55**(189), 43–52.
- Smedsrud, L.H. 2001. Frazil-ice entrainment of sediment: large-tank laboratory experiments. *J. Glaciol.*, **47**(158), 461–471.
- Smedsrud, L.H. and R. Skogseth. 2006. Field measurements of Arctic grease ice properties and processes. *Cold Reg. Sci. Technol.*, **44**(3), 171–183.
- Smith, S.D. 1988. Coefficients for sea surface wind stress, heat flux, and wind profiles as a function of wind speed and temperature. *J. Geophys. Res.*, **93**(C12), 15,467–15,472.
- Steiner, N. 2001. Introduction of variable drag coefficients into sea-ice models. *Ann. Glaciol.*, **33**, 181–186.
- Vancoppenolle, M., T. Fichefet, H. Goosse, S. Bouillon, G. Madec and M.A. Morales Maqueda. 2010. Simulating the mass balance and salinity of Arctic and Antarctic sea ice. 1. Model description and validation. *Ocean Model.*, **27**(1–2), 33–53.
- Wadhams, P. and J.P. Wilkinson. 1999. The physical properties of sea ice in the Odden ice tongue. *Deep-Sea Res. II*, **46**(6–7), 1275–1300.
- Winsor, P. and G. Björk. 2000. Polynya activity in the Arctic Ocean from 1958–1997. *J. Geophys. Res.*, **105**(C4), 8789–8803.